Short Communications

Interaction Between a Linearly Polarized Electromagnetic Plane and a Double Spherical Shell

DANIEL L. DAWES AND JERRY W. GASKILL

Abstract—**An exact solution inside, outside, and within two arbitrary concentric spherical shells is presented for an impinging monochromatic linearly polarized electromagnetic wave. Specifically, the solution was found for a double-shell spherical acrylic plastic enclosure irradiated with 2450-MHz microwaves. The enclosure is used as an environmentally controlled exposure chamber for experimental animals during microwave irradiation. The analysis shows that an air foamed material, such as styrofoam, would be a better material than either Plexiglas[1] or Teflon, provided it is sufficiently durable.**

Introduction

An animal exposure chamber made of concentric Plexiglas spheres has been developed for use in our laboratory to study the effects of microwave exposure on various animals (Fig. 1). Composition, velocity, humidity, total pressure, and temperature of the atmosphere within the spherical chamber are controlled and monitored, and various physiological responses of the animal are recorded during microwave irradiation. The exposure chamber is wholly contained in an anechoic microwave chamber and the experimental animal is subjected to 2450-MHz microwaves emanating from a Varian microwave generator.

The problem of scattering and absorption by spheres illuminated by a plane wave has been of interest to a large number of people for many years. The earliest substantial published discussion about the problem is Mie's in 1908 [4]. Since that time a number of investigations have contributed to the analysis of the problem [1] and the exact solution has become part of standard textbook material [3], [6]. The numerical reduction for any point in space in or around the spheres can be easily calculated using modern computers [2], [5].

Our problem was to analyze the electromagnetic field structure within a set of concentric Plexiglas spheres. The model of two concentric lossy dielectric shells illuminated by a plane wave was chosen as an approximation to the actual situation where flanges, internal and external supports, tubes, and a slightly nonplanar exposure field complicate the scattering pattern.

The solution to the model can be solved exactly using vector multipole expansions. The method is applicable to spheres of arbitrary sizes, electric and magnetic parameters, and polarization of the incident wave. The method can be generalized to an arbitrary number of concentric spheres [5].

The analysis presented here follows that of Chu *et al.* [2] with the exception that in this case the problem is worked in rationalized MKSA units; a linearly polarized plane wave is considered rather than a circularly polarized one and four rather than two concentric layers are considered.

The Analytical Solution

As always, the starting point is Maxwell's relations. In MKSA units they are

$$\nabla \cdot \boldsymbol{D} = \rho$$

$$\nabla \times \boldsymbol{H} = j + \frac{\partial \boldsymbol{D}}{\partial t}$$

Manuscript received October 29, 1971; revised January 20, 1972.

D. L. Dawes was with the Environmental Protection Agency, Twinbrook Research Laboratory, Rockville, Md. 20852. He is now at the California Institute of Technology, Pasadena, Calif.

J. W. Gaskill is with the Environmental Protection Agency, Twinbrook Research Laboratory, Rockville, Md. 20852.

[1] Plexiglas is a trade name of Rohm and Haas, Philadelphia, Pa.

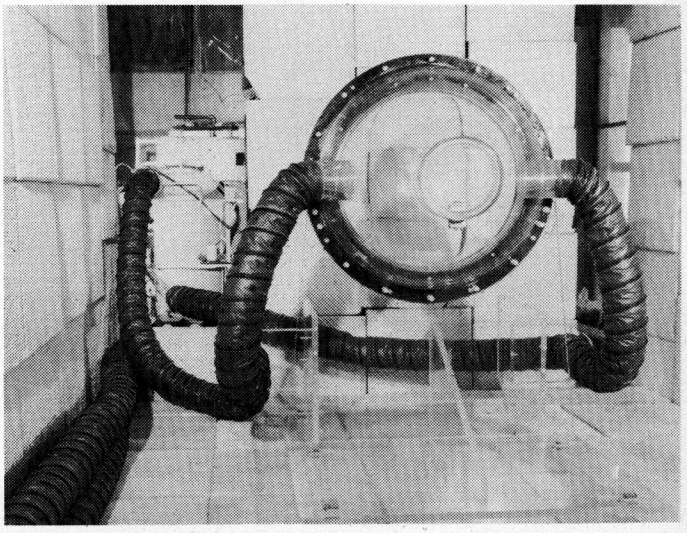

Fig. 1. Double-walled Plexiglas hemispheres form an environmental chamber for biological exposures to microwaves in a controlled environment (temperature, humidity, and gas composition). These microwaves are provided to the inner sphere by the accordion pipes; access is through a porthole in the rear, as seen in this view.

$$\nabla \cdot \boldsymbol{B} = 0$$

$$\nabla \times \boldsymbol{E} = -\frac{\partial \boldsymbol{B}}{\partial t}.$$

For linear, homogeneous, and isotropic media in the presence of harmonic fields, Maxwell's relations produce the vector wave equation for the electric and magnetic field vectors, $\boldsymbol{E}$ and $\boldsymbol{H}$, respectively (assuming $\rho = 0$ everywhere):

$$\nabla^2 \boldsymbol{V} + k^2 \left(\mu\epsilon + \frac{i\mu\sigma}{\epsilon_0 \omega}\right) \boldsymbol{V} = 0$$

where

$$\boldsymbol{V} = \boldsymbol{E} \quad \text{or} \quad \boldsymbol{H}$$

and

k^2 $= \omega^2/c^2$;
μ, ϵ relative real magnetic permeability and dielectric constant, respectively;
σ conductivity;
ϵ_0 dielectric constant of free space 8.85×10^{-12} f/m;
c velocity of light;
i $= \sqrt{-1}$.

Each rectangular component satisfies Helmholtz's equation so that the general solution is

$$V = \sum_{l=0}^{\infty} \sum_{m=-l}^{l} \left[A_{lm}^1 h_l^1(\kappa r) + A_{lm}^2 h_l^2(\kappa r)\right] Y_{lm}(\theta, \varphi)$$

where

A_{lm}^1, A_{lm}^2 constant vectors;
h_l^1, h_l^2 spherical Hankel functions;
$Y_{lm}(\theta, \varphi)$ spherical harmonic functions;
κ^2 $= k^2(\mu\epsilon + i\mu\sigma/\epsilon_0\omega)$.

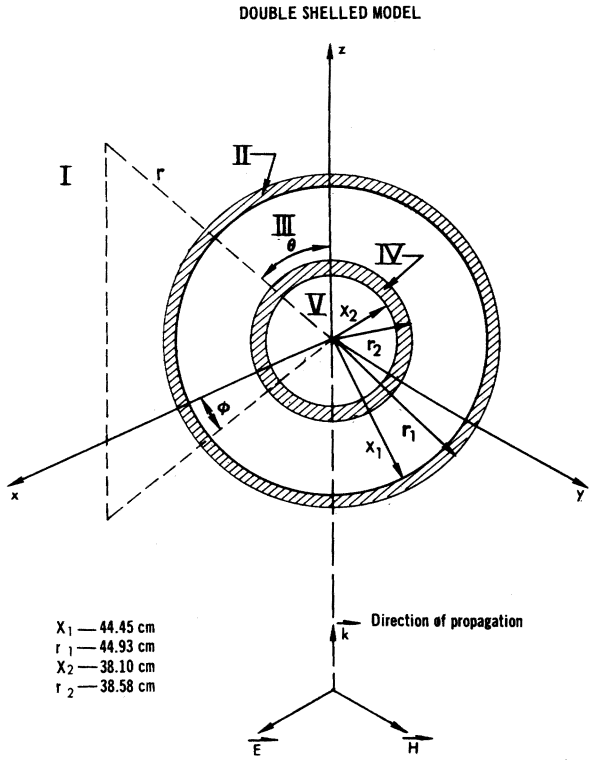

Fig. 2. Reference frame in spherical and Cartesian coordinates.

The vector constants are not entirely arbitrary since, in the absence of sources, the equations

$$\nabla \cdot H = 0$$
$$\nabla \cdot E = 0$$

constrain the constants.

Following the steps explained by Jackson [3, sec. 16.2], the general solutions take the form

$$E = \sum_{l=0}^{\infty} \sum_{m=-l}^{l} \left[a_{lm} g_l(\kappa r)\, LY_{lm}(\theta, \varphi) + \frac{b_{lm}}{(\sigma - i\omega\epsilon)} \nabla \times \{ f_l(\kappa r)\, LY_{lm}(\theta, \varphi) \} \right]$$

$$H = \sum_{l=0}^{\infty} \sum_{m=-l}^{l} \left[b_{lm} f_l(\kappa r)\, LY_{lm}(\theta, \varphi) - \frac{i a_{lm}}{\omega\mu} \nabla \times \{ g_l(\kappa r)\, LY_{lm}(\theta, \varphi) \} \right]$$

where a_{lm} and b_{lm} are scalar constants. The functions g_l and f_l take the form

$$g_l(\kappa r) = c_1 h_l^1(\kappa r) + c_2 h_l^2(\kappa r)$$
$$f_l(\kappa r) = d_1 h_l^1(\kappa r) + d_2 h_l^2(\kappa r)$$

with c_1, c_2, d_1, and d_2 being scalar constants and the vector operator L defined by

$$L = \frac{1}{i}(r \times \nabla).$$

A plane wave can be expressed in spherical coordinates by transforming

$$E = \hat{x} E_0 e^{ikz}$$
$$H = \frac{-i}{\omega\mu} \nabla \times E = \hat{y}\, \frac{k}{\omega\mu} E_0 e^{ikz}$$

into the form

$$E = E_0 \sum_{l=1}^{\infty} i^l \sqrt{\pi(2l+1)} \left[j_l(kr)\, X_{l,\pm 1} \mp \frac{1}{k} \nabla \times \{ j_l(kr)\, X_{l,\pm 1} \} \right]$$

$$H = E_0 \sum_{l=1}^{\infty} i^l \sqrt{\pi(2l+1)} \left[\pm i \sqrt{\frac{\epsilon_0}{\mu_0}}\, j_l(kr)\, X_{l,\pm 1} - \frac{i}{\omega\mu_0} \nabla \times \{ j_l(kr)\, X_{l,\pm 1} \} \right]$$

using steps similar to those used by Jackson [3, sec. 16.8].

$$X_{l,\pm 1} = \frac{1}{\sqrt{l(l+1)}}\, LY_{l,\pm 1}(\theta, \varphi).$$

The ± notation is used here as an implicit sum, e.g.,

$$f = a_{\pm} z \mp b_{\pm}$$

means

$$f = a_+ z - b_+ + a_- z + b_-.$$

Now consider the problem at hand. The double-shelled chamber divides space into five regions, as pictured in Fig. 2. The origin is at the center of the concentric spheres.

Chu *et al.* [2] describe the field in region I as the sum of

$$E = E_0 \sum_{l=1}^{\infty} i^l \sqrt{\pi(2l+1)} \left[j_l(kr)\, X_{l,\pm 1} \mp \frac{1}{k} \nabla \times \{ j_l(kr)\, X_{l,\pm 1} \} \right]$$

$$H = E_0 \sum_{l=1}^{\infty} i^l \sqrt{\pi(2l+1)} \left[\pm c \sqrt{\frac{\epsilon_0}{\mu_0}}\, j_l(kr)\, X_{l,\pm 1} - \frac{i}{\omega\mu_0} \nabla \times \{ j_l(kr)\, X_{l,\pm 1} \} \right]$$

and the scattered field

$$E_{sc} = E_0 \sum_{l=1}^{\infty} i^l \sqrt{\pi(2l+1)} \left[\alpha_l h_l^1(kr)\, X_{l,\pm 1} \mp \frac{\beta_l}{k} \nabla \times \{ h_l^1(kr)\, X_{l,\pm 1} \} \right]$$

$$H_{sc} = \sqrt{\frac{\epsilon_0}{\mu_0}} E_0 \sum_{l=1}^{\infty} i^l \sqrt{\pi(2l+1)} \left[\pm i h_l^1(kr)\, X_{l,\pm 1}\, \beta_l - \frac{\alpha_l i}{k} \nabla \times \{ h_l^1(kr)\, X_{l,\pm 1} \} \right]$$

where α_l and β_l are constants to be determined by the boundary conditions.

In region II

$$E_{II} = E_0 \sum_{l=1}^{\infty} i^l \sqrt{\pi(2l+1)} \left[(A^1 h_l^1 + A^2 h_l^2)\, X_{l,\pm 1} \mp \frac{1}{\kappa_1} \nabla \times \{ (B^1 h_l^1 + B^2 h_l^2)\, X_{l,\pm 1} \} \right]$$

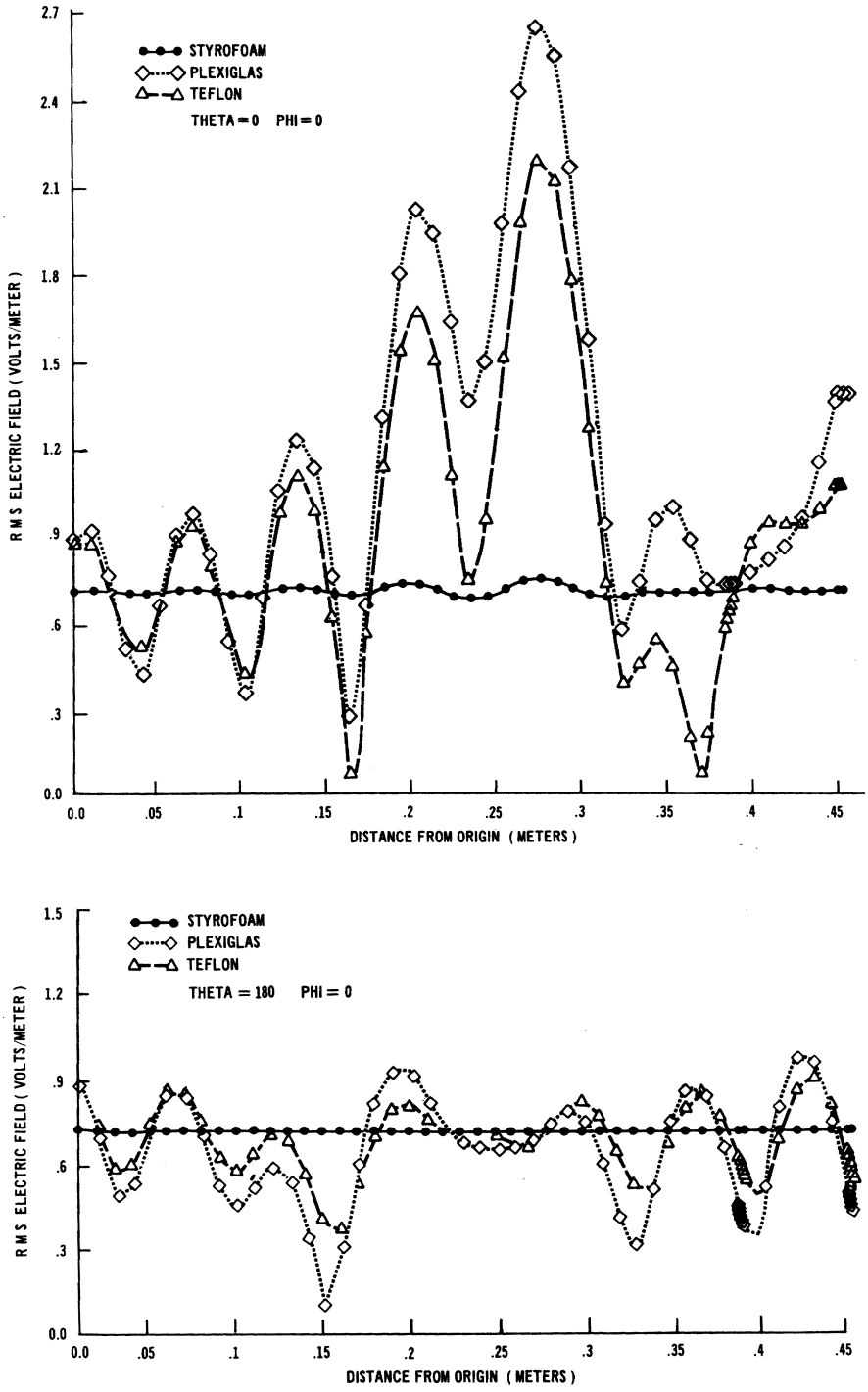

Fig. 3. Plot of the rms electric field in MKSA units (volts/meter) on four rays from the origin to the outside surface of the outer shell. In the air spaces a point is computed every centimeter, while inside the shells themselves it is computed every 2 mm. The rays are the positive x, y, and z axes and the negative z axis. Each plot compares the standing wave pattern of identical spherical shells made alternatively out of Plexiglas, Teflon, and styrofoam. A plane wave irradiation of 2450 MHz is assumed throughout.

and

$$H_{II} = E_0 \sum_{l=1}^{\infty} i^l \sqrt{\pi(2l+1)}\, \frac{\kappa_1}{\omega\mu} \left[\pm i(B^1 h_l^1 + B^2 h_l^2)\, X_{l,\pm 1} - \frac{i}{\kappa_1} \nabla \times \{(A_l^1 h_l^2 + A_l^2 h_l^2)\, X_{l,\pm 1}\} \right].$$

This type of function is repeated for regions III and IV with different coefficients C^1, C^2, D^1, D^2, F^1, F^2, G^1, and G^2.

In region V

$$E_V = E_0 \sum_{l=1}^{\infty} i^l \sqrt{\pi(2l+1)} \left[M^1 j_l(kr)\, X_{l,\pm 1} \mp \frac{1}{k} \nabla \times \{M^2 j_l(kr)\, X_{l,\pm 1}\} \right]$$

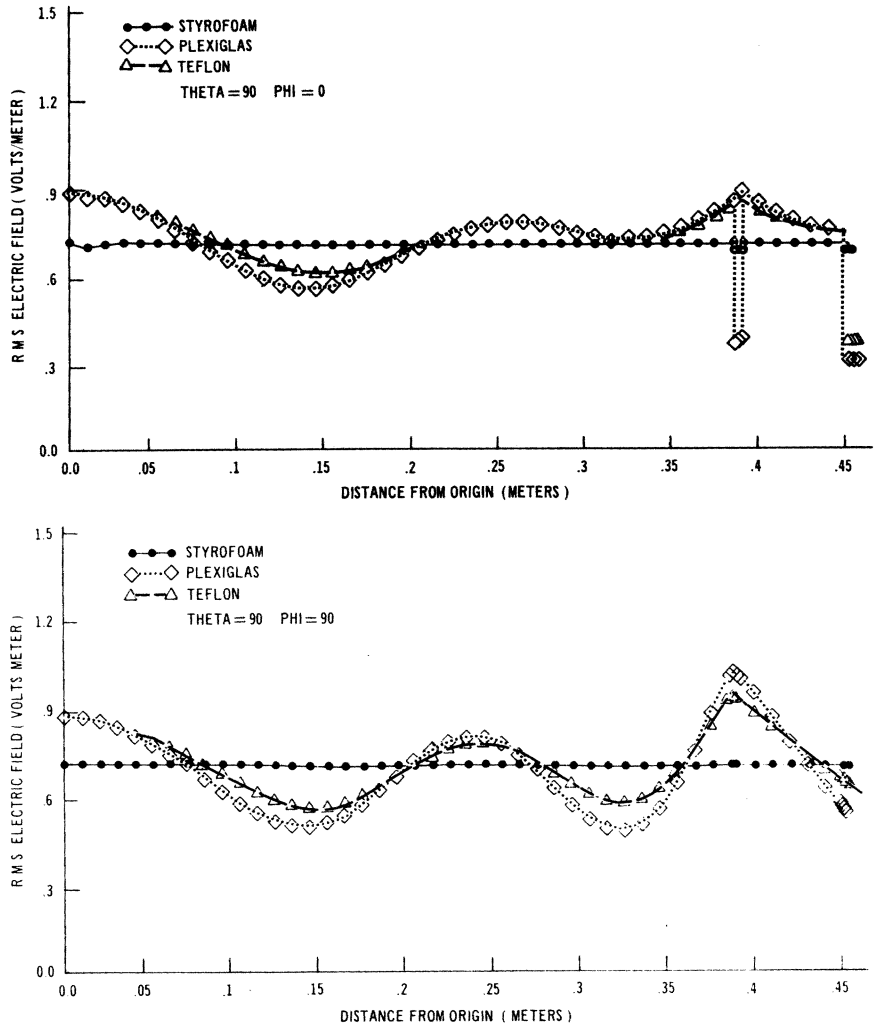

Fig. 4. Plot of the rms electric field in MKSA units (volts/meter) on four rays from the origin to the outside surface of the outer shell. In the air spaces a point is computed every centimeter, while inside the shells themselves it is computed every 2 mm. The rays are the positive x, y, and z axes and the negative z axis. Each plot compares the standing wave pattern of identical spherical shells made alternatively out of Plexiglas, Teflon, and styrofoam. A plane wave irradiation of 2450 MHz is assumed throughout.

$$H_V = \frac{E_0 k}{\omega \mu_0} \sum_{l=1}^{\infty} i^l \sqrt{\pi(2l+1)} \left[\pm i M^2 j_l(kr) X_{l,\pm 1} - \frac{i}{k} \nabla \times \{M^1 j_l(kr) X_{l,\pm 1}\} \right].$$

The 8 boundary conditions

$$\hat{r} \times (E_n - E_{n+1})_b = 0 \qquad \nabla \cdot H = 0$$
$$\hat{r} \times (H_n = H_{n+1})_b = 0 \qquad \nabla \cdot D = 0$$

determine the 16 coefficients. The solution to the wave equation in spherical coordinates is entirely transverse to the radial vector $\hat{r}$. The vectors E and H, therefore, are always transverse to the radial vector $\hat{r}$ and can be expressed as 2 mutually orthogonal vectors $X_{l,\pm 1}$ and $\hat{r} \times X_{l,\pm 1}$ [2]. At each interface the tangential boundary conditions on E and H expressed above produce 4 linear scalar equations; these equations are derived from the coefficients of $X_{l,\pm 1}$ and $\hat{r} \times X_{l,\pm 1}$ in the boundary conditions for E and H. In this problem there are 4 interfaces, the inside and outside surfaces of both shells. The 4 scalar equations from each of the 4 surfaces make up the 16 linearly independent equations needed to solve the 16 unknowns.

For the interface $r = r_1$ the condition on E yields

$$(j_l + \alpha_l h_l^1)_{r_1,k} = (A_l^1 h_l^1 + A_l^2 h_l^2)_{r_1,\kappa}$$

$$\frac{1}{k}\left(\frac{\partial}{\partial r}\{r j_l + B_l r h_l^1\}\right)_{r_1,k} = \frac{1}{\kappa}\frac{\partial}{\partial r}(r\{B_l^1 h_l^1 + B_l^2 h_l^2\})_{r_1,\kappa}$$

and the condition on H yields

$$\sqrt{\frac{\epsilon_0}{\mu_0}}(j_l + B_l h_l^1)_{r_1,k} = \frac{\kappa}{\omega\mu}(B_l^1 h_l^1 + B_l^2 h_l^2)_{r_1,\kappa}$$

$$\frac{1}{\mu_0}\left(\frac{\partial}{\partial r} r\{j_l + \alpha_l h_l^1\}\right)_{r_1,k} = \frac{1}{\mu}\left(\frac{\partial}{\partial r} r\{A_l^1 h_l^1 + A_l^2 h_l^2\}\right)_{r_1,\kappa}.$$

Similar equations are produced for each of the other 3 interfaces. The result is 16 unknowns and 16 linear algebraic equations, which separate into 2 independent 8 X 8 matrices and can be easily solved by matrix algebra.

The computer programs required for the numerical reductions were originally written for a computer having a large memory size. These programs have been modified to run on a smaller computer by using program overlay techniques and auxiliary disk and tape storage.

Thus the computational technique used to produce the results described in this paper is available to a larger number of potential users. In particular, these programs can now be run on an IBM 360/30 computer having 64k bytes of core storage and using the disk operating system.

TABLE I
RELATIVE DIELECTRIC CONSTANT AND CONDUCTIVITY OF ACRYLIC, STYROFOAM, AND TEFLON AT 3 GHz

	K	(mho/m)
Acrylic Plastic (Plexiglas)	2.60	0.0032
Styrofoam	1.03	0.000014
Teflon	2.10	0.000043

RESULTS

In Figs. 3 and 4 the root-mean-square electric field is plotted against the radius inside of three double-shelled spherical chambers made of Plexiglas, Teflon, and styrofoam, respectively. An incident plane wave polarized with E in the $\hat{x}$ direction with an amplitude of 1 V/m or 0.707 rms V/m, and with a frequency of 2450 MHz has been assumed throughout. The plane wave is moving from the negative $\hat{z}$ direction to the positive $\hat{z}$ direction. The four plots compare the standing waves inside the chamber along the positive axes and along the negative $\hat{z}$ axis from the origin through the inner shell at 38.1–38.576 cm to the outer shell at 44.45–44.926 cm.

The values taken for the dielectric parameters of Plexiglas, Teflon, and styrofoam are listed in Table I and were derived from values given in [7].

The Teflon and Plexiglas double-walled spherical chambers set up very similar standing patterns despite the nearly 20-percent difference in dielectric constant and two orders of magnitude difference in conductivity. Both have a hot spot near the rear of the chamber that is more than three times greater than the magnitude of the incident electric field strength.

As expected, an rms standing wave pattern with a periodicity of a half wavelength is set up along the direction of propagation. Transverse to the direction of propagation, an rms standing wave pattern of approximately a full wavelength is calculated. We take this to be a peculiar artifact of the geometry of the chamber.

The plots for styrofoam show a comparatively small standing wave pattern of the same general form. Again the hot spot is near the rear of the inner chamber, but is less than 6 percent higher than the incident field strength.

DISCUSSION

The application of this analysis has been concerned with the standing wave patterns set up in a double-walled Plexiglas spherical chamber in which small mammals are irradiated by 2450-MHz CW electromagnetic radiation. The purpose of the chamber was to contain and insulate a controlled environment. We have demonstrated that significant standing wave patterns are to be expected inside the chamber along the beam axis. Had the choice of material been Teflon rather than Plexiglas, little improvement would have resulted. This analysis shows that styrofoam would be a much better material for constructing exposure cells for biological targets if it can satisfy requirements for mechanical strength and durability. Any nonlossy foamed material may be an improvement over Plexiglas for such exposure chambers, even foamed Plexiglas.

The closer the dielectric constant approaches unity, the closer, of course, the material will electromagnetically match or blend with air. Wide variations of conductivity within the magnitudes used in this problem have little effect on the suitability of the material as a container or animal constrainer for bio-effects research at 2450 MHz. We would expect to draw analogous conclusions for animal constrainers of any shape that are intended for microwave exposure in bio-effects research.

ACKNOWLEDGMENT

The authors would like to thank A. R. Shapiro of the Rand Corporation, Santa Monica, Calif., for making the original computer programs available to us, Miss Judy Kuhn for preparing the programs used to plot the results, and Mrs. Pat Nash for typing the manuscripts.

REFERENCES

[1] D. E. Barrick, *Radar Cross Section Handbook*, vol. 1, G. T. Ruck, Ed. New York: Plenum, 1970, pp. 202–204.
[2] G. Chu, D. G. Dudley, and T. W. Bristol, "Interaction between an electromagnetic plane wave and a spherical shell," *J. Appl. Phys.*, vol. 40, no. 10, pp. 3904–3914, 1969.
[3] J. D. Jackson, *Classical Electrodynamics*. New York: Wiley, 1967, ch. 16, p. 538.
[4] G. Mie, "Beitrage zur optik truber medien. Speziell holloidaler metalosungen," *Ann. Phys.* (Leipzig), vol. 25, p. 377, 1908.
[5] A. R. Shapiro, R. F. Lutomirski, and H. T. Yura, "Induced fields and heating within a cranial structure irradiated by an electromagnetic plane wave," *IEEE Trans. Microwave Theory Tech.*, vol. MTT-19, pp. 187–196, Feb. 1971.
[6] J. A. Stratton, *Electromagnetic Theory*. New York: McGraw-Hill, 1941, ch. VII, pp. 392–420.
[7] H. Westman, Ed., *Reference Data for Radio Engineers*, 5th ed. Indianapolis, Ind.: Howard W. Sams & Co., 1969, pp. 28–31.

A Multipurpose Electronic Filter and Integrating Level Detector

MARC S. WEISS, JOHN S. SOBOLEWSKI, ASSOCIATE MEMBER, IEEE, AND ROBERT DRURY

Abstract—**A multipurpose electronic filter and integrating level detector suitable for electroencephalographic (EEG) and electromyographic recording and analysis is described. It uses solid-state components and is easily constructed. An application of the device in the detection of slow wave sleep (SWS) potentials is given.**

I. INTRODUCTION

There are instances in the EEG laboratory when data are reduced on-line either to quantify certain spectral properties or to manipulate experimental conditions (e.g., the "bio-feedback" procedure in [1], [2]). The device described here is a solid-state general-purpose filter, rectifier, integrator, and level detector using inexpensive integrated-circuit operational amplifiers. It provides flexible and highly reliable performance characteristics suitable for on-line use.

II. CIRCUIT DESCRIPTION

The device consists of five sections as shown in Fig. 1. Each section can function independently or in conjunction with other sections. The sections are as follows.

A. Low-Pass Filter

This is a unity-gain two-stage Butterworth filter (maximally flat frequency response). The high frequency attenuation is approximately 24 dB/octave (80 dB/decade). With the capacitor values shown, the cutoff frequency f_{CL} depends upon R_L and is given by

$$f_{CL} = 1/R_L \tag{1}$$

where f_{CL} is in hertz and R_L is in megohms. R_L can be fixed or switch selected for a variable cutoff point. R_3 is used to trim the output dc offset to 0 V.

B. High-Pass Filter

The high-pass filter can be used alone or in conjunction with the low-pass filter to form a bandpass filter. Its bandpass and cutoff character-

Manuscript received January 10, 1972. This work was supported in part by the State of Washington under Initiative Measure 171 and in part by the Washington State University Graduate School Research funds.
M. S. Weiss is with the Department of Psychology and the Computing Center, Washington State University, Pullman, Wash. 99163.
J. S. Sobolewski is with the Departments of Computer Science and Electrical Engineering and the Computing Center, Washington State University, Pullman, Wash. 99163.
R. Drury is with the Department of Psychology, Washington State University, Pullman, Wash. 99163.